Synthesis of Highly Monodisperse Silver Nanoparticles from AOT Reverse Micelles: A Way to 2D and 3D Self-Organization

A. Taleb,[†] C. Petit,[†,‡] and M. P. Pileni*[,†,‡]

Laboratoire SRSI, URA CNRS 1662, Universite P. et M. Curie Bât F, 4 Place Jussieu, 75005 Paris, France, and CEA-Saclay, DSM-DRECAM Service de Chimie Moléculaire, 91 191 Gif sur Yvette Cedex, France

Received September 30, 1996. Revised Manuscript Received January 27, 1997[⊗]

A simple method is used to prepare highly monodispersed silver nanoparticles in the liquid phase, which starts from an initial synthesis in functionalized AOT reverse micelles. To narrow the particle size distribution from 43% to 12.5% in dispersion, the particles are extracted from the micellar solution. The size-selected precipitation method is used. The decrease in polydispersity of the silver nanoparticles is followed by transmission electron microscopy, by UV−vis spectroscopy, and by small-angle X-ray scattering. The nanocrystallites dispersed in hexane are deposited on a support. A monolayer made of nanoparticles with spontaneous hexagonal organization is observed. The immersion of the support on the solution yields to the formation of organized multilayers arranged as microcrystal in a face-centered cubic structure.

Introduction

Nanochemistry is emerging as a new field of the solid-state chemistry since the early 1980s.[1] Chemists have tried to obtain materials in nanometer scales and have succeeded to drastically reduce the characteristic size of inorganic particles.

Colloidal assemblies such as reverse micelles are good candidates to reduce the size of crystallites. From the initial work on cadmium sulfide quantum dots,[2] numerous publications have appeared on semiconducting, metallic, and/or magnetic nanoparticles to study the quantum size effect on optical, catalytic, or magnetic properties.[3]

Chemists are currently trying to change at a macroscopic scale the shape of these new materials[4,5] and to organize them.[6,7] The creation of perfect nanometer-scale crystallites identically replicated with a long-range order in a state that can be manipulated and understood as pure macromolecular substance is an ultimate challenge in the actual materials research. To develop their application as novel optical and electronic materials, it is crucial to control the spatial arrangement of these nanoparticles in 2D or 3D arrays. Usually external forces are used to organize the particles.[8−10] Recently, however, spontaneous arrangement with semiconductor as Ag_2S[7] and CdSe[6] or metallic particles as gold or silver[11] has been reported. FCC arrangement of particles of different sizes has been characterized for microcrystals of silver sulfide nanoparticles.[7] Similar results were also reported in the case of CdSe nanoparticles[6] or gold metallic nanoparticles.[11]

In a previous paper,[12] we have shown that AOT reverse micelles can be used as a microreactor to control the size of silver metallic particles. The use of functionalized surfactant prevents the oxidation of the silver. This permits the synthesis of silver metallic particles at room temperature under air. The size distribution of the nanocrystallites remains rather large.

In the present paper, the size-selected precipitation technique has been used to decrease the polydispersity. This favors the organization of silver particles in 2D and 3D supperlattices.

Experimental Section

Products. AOT was purchased from Sigma. Isooctane, hexane, and pyridine were purchased from Fluka. Hydrazine and dodecanethiol were obtained from Prolabo (France) and Janssen chemicals respectively. The materials were not further purified.

[†] Laboratoire SRSI.
[‡] CEA-Saclay.
* To whom correspondence should be addressed.
[⊗] Abstract published in *Advance ACS Abstracts,* March 15, 1997.

(1) (a) Ozin, G. A. *Adv. Mater.* **1992**, *4*, 612; (b) *Science* **1996**, *271*, 920−941.
(2) (a) Lianos, P.; Thomas, J. K. *Chem. Phys. Lett.* **1986**, *125*, 299. (b) Petit, C.; Pileni, M. P. *J. Phys. Chem.* **1988**, *92*, 2282.
(3) For review, see: (a) Pileni, M. P. *Langmuir*, in press. (b) Pileni, M. P. *J. Phys. Chem.* **1993**, *97*, 6961. (c) Wang, Y. *Acc. Chem. Res.* **1991**, *24*, 133. (d) Fendler, J. H. *Chem. Rev.* **1987**, *87*, 877.
(4) (a) Lisiecki, I.; Billoudet, F.; Pileni, M. P. *J. Phys. Chem.* **1996**, *100*, 4160. (b) Tanori, J.; Pileni, M. P. *Adv. Mater.* **1995**, *7*, 862.
(5) Esumi, K.; Matshushisa, K.; Torigoe, K. *Langmuir* **1995**, *11*, 3285
(6) Murray, C. B.; Kagan, C. R.; Bawendi, M. G. *Science* **1995**, *270*, 1335
(7) Motte, L.; Billoudet, F.; Pileni, M. P. *J. Phys. Chem.* **1995**, *99*, 16425.
(8) Giersig, M.; Mulvaney, P. *Langmuir* **1993**, *9*, 3408.
(9) (a) Dabbousi, B. O.; Murray, C. B.; Rubner, M. F.; Bawendi, M. G. *Chem. Mater.* **1994**, *6*, 216. (b) Kotov, N. A.; Meldrum, F. C.; Fendler, J. H. *J. Phys. Chem.* **1994**, *98*, 8827. (c) Yi, K. C.; Sanchez-Mendieta, V.; Castañares, R. L.; Meldrum, F. C.; Wu, C.; Fendler, J. H. *J. Phys. Chem.* **1995**, *99*, 9869.
(10) Francis, G. M.; Kuipers, L.; Cleaver, J. R. A.; Palmer, R. E. *J. Appl. Phys.* **1996**, *79*, 2942.
(11) (a) Whetten, R. L.; Khoury, J. T.; Alvarez, M. M., Murthy, S.; Vezmar, I.; Wang, Z. L.; Cleveland, C. C.; Luedtke, W. D.; Landman, U. *Adv. Mater.* **1996**, *8*, 429. (b) Brust, M.; Bethell, D.; Schiffrin, D. J.; Kiely, C. J. *Adv. Mater.* **1995**, *7*, 9071.
(12) Petit, C.; Lixon, P.; Pileni, M. P. *J. Phys. Chem.* **1993**, *97*, 12974.

S0897-4756(96)00513-3 CCC: $14.00

Silver bis(2-ethylhexyl)sulfosuccinate, Ag(AOT), has been prepared as described previously.[12,13]

The concentrations given in the text are the overall concentrations.

All the experiments were done at room temperature without any specific protection.

Silver metallic nanocrystallites synthesized in situ, in reverse micelles, are stable over months, even in the presence of oxygen.[12]

Apparatus. Absorption spectra were recorded on a conventional Varian Cary 1 spectrophotometer (in 1 or 2 mm cuvettes).

For the transmission electron microscopy (TEM) measurements a drop of the solution was placed onto a carbon-coated copper grid. After evaporation of the solvent, micrographs were recorded on a transmission electron microscope (JEOL 100CX). Tilt experiments were done on a JEOL 200 CX electron microscope operating at 200 keV and equipped with a double tilt holder.

Histograms. The histograms of the nanocrystallites were obtained by measuring the diameter D_i of the particles from five micrographs on different parts of the grid (the magnification is 160 000). Depending on the experimental condition, the number of particles measured, n, range from 500 to 1000. The standard deviation, σ, was calculated from the experimentally determined distributions:

$$\sigma = \{[\sum n_i(D_i - D)^2]/[n - 1]\}^{1/2}$$

where D is the average diameter.

SAXS Experiments. The scattered X-ray intensity at low angles was measured from 0.025 to 0.5 $Å^{-1}$ (which corresponds to a resolution in real space from 10 to 250 Å), using a high-flux camera and Cu Kα radiation (1.54 Å). The experimental arrangement is described elsewhere[14] as well as the scattering patterns analysis.[15]

The good agreement between the diameter of the particles deduced from different representations of the scattered intensity (i.e., Porod's or Guinier's plots) supports the scatter of spheres. This can be further confirmed by a simulation of the scattering patterns carried out using the known composition of the sample, silver, and hexane and the estimated radius. In this simulation the polydispersity can be estimated as a Gaussian distribution of the particle size centered on the estimated radius, R_{fit}.[16]

Results and Discussion

Synthesis of Silver Particles in Reverse Micelles. The preparation of colloidal silver particles is achieved by mixing two AOT reverse micellar solutions having the same water content (i.e., molar ratio $W = [H_2O]/[AOT] = 40$). The first is made with 30% Ag(AOT), 70% Na(AOT) and the second with N_2H_4 with 100% of Na(AOT). The overall concentration of hydrazine is 7×10^{-2} M. This corresponds, at $W = 40$, to an average number of hydrazine per micelle equal to 700. In the first approximation, because of the large amount of hydrazine per micelle, it can be assumed that most of silver ions solubilized in the water pool are reduced.

Figure 1 (solid line) shows the UV−visible absorption spectrum obtained immediately after mixing the two micellar solutions. A well-defined surface plasmon peak characterized by a maximum centered at 400 nm is observed. According to the calculated absorption spectrum,[12] this is attributed to nanosized metallic silver particles. Further characterization is obtained by TEM. The corresponding electron microscopy and histogram (Figure 2A) show formation of spherical particles with an average diameter equal to 3.4 nm and a polydispersity of 43% (Table 1). The formation of silver metallic particles is confirmed by electron diffraction. It reveals a crystalline order. Spacings are observed at 2.36, 2.04, 1.44, 1.22, 1.18, and 0.94 Å, which are all within 2% of the values reported for the 111, 200, 220, 311, 222, and 331 FCC metallic silver reflection, respectively.[17]

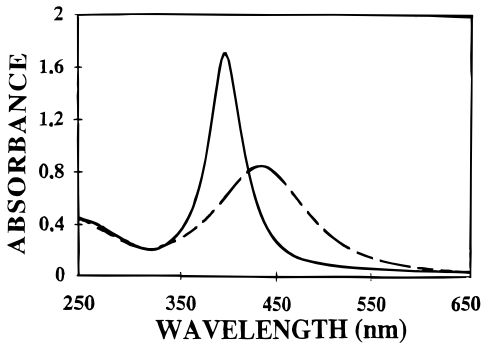

Figure 1. UV−visible absorption spectra of silver colloidal solution after synthesis in reverse micelles (—) and after addition of dodecanethiol in the micellar solution (- -).

Table 1. Size Distribution of Silver Nanosized Particles at Different Steps of the Selection Process: After Synthesis in Reverse Micelles, after Extraction by Dodecanethiol, after Size-Selected Precipitation (Fractionation on the First Fraction)

sample	av diam (nm)	std dev (nm)	polydispersity (%)
silver in micelles	3.4	1.4	43
silver after extraction	3.5	1.3	37
silver after SSP	4.1	0.5	12.5

Extraction of Silver Particles from Micellar Media. The particles are extracted from micelles by adding dodecanethiol to the solution (1 μL for 1 cm^3). Due to the strong affinity of the SH headgroup for the noble metal[18] there is a selective reaction of the dodecanethiol on the silver particles. The attachment of dodecanethiol on the silver particles can be monitored by UV−vis spectroscopy: Figure 1 (dotted line) shows the drastic decrease in the extinction coefficient of the plasmon band after dodecanethiol addition, whereas below 300 nm, no change in the UV absorption is observed. This strong decrease in the intensity and the red-shift of the maximum observed in the absorption spectrum for coated particles are due to a change in the free electron density. This induces changes in the surface plasmon band of silver particles[19] and yields a variation of the width and maximum of the plasmon band absorption.[19,20] Similar behavior has been observed from NaSH addition to silver colloids in aqueous solution.[21]

Ethanol addition to the micellar solution induces flocculation of the silver dodecanethiol coated particles.

(13) Petit, C.; Lixon, P.; Pileni, M. P. *J. Phys. Chem.* **1990**, *94*, 1598.
(14) Né, F.; Gazeau, D.; Lambard, J.; Lesieur, P.; Zemb, T. *J. Appl. Cryst.* **1993**, *26*, 763.
(15) Petit, C.; Bommarius, A. S.; Pileni, M. P. Hatton, A. T. *J. Phys. Chem.* **1992**, *96*, 2929.
(16) Pitré, F.; Regnault, C.; Pileni M. P. *Langmuir* **1993**, *9*, 2855.
(17) *JCPDS*, International Centre for Diffraction Data, No. 4-783.
(18) Li, W.; Virtanen, J. A.; Penner, R. M. *Langmuir* **1995**, *11*, 4361.
(19) Charlé, K. P.; Frank, F.; Schulze, W. *Ber. Bunsen-Ges. Phys. Chem.* **1984** *88*, 354.
(20) Kreibig, U. *J. Phys. F: Met. Phys.* **1974**, *4*, 999.
(21) Mulvaney, P.; Linnert, T.; Henglein, A. *J. Phys. Chem.* **1991**, *95*, 5, 7843.

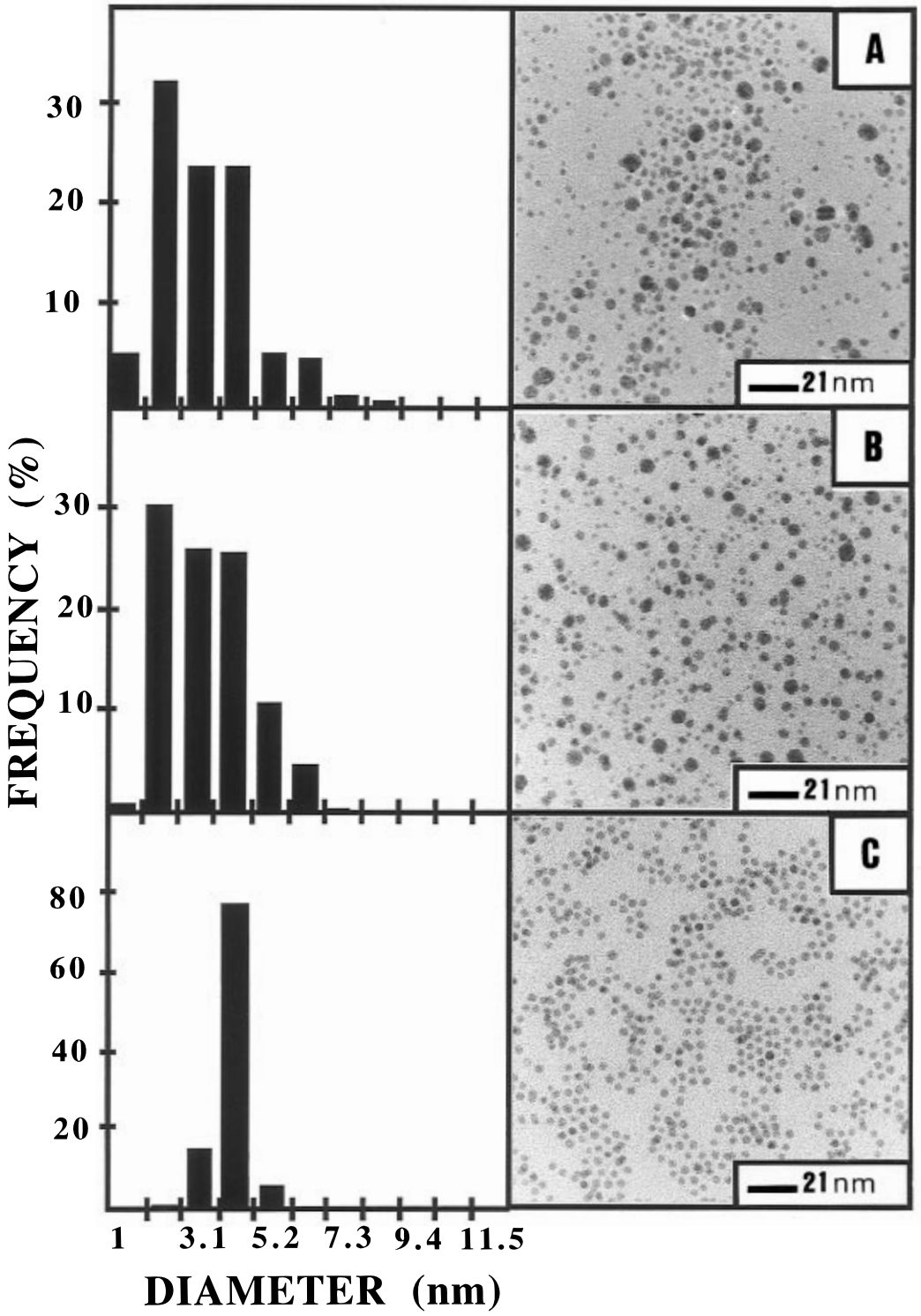

Figure 2. TEM micrograph and histograms of size of silver particles: in reverse micelle (A), after extraction (B), and at the end of the size-selected precipitation process (see text)(C).

Then, the solution is filtered. The precipitate is easily redispersed in hexane. After extraction, the size distribution (Table 1) is reduced (Figure 2B) compared to what it has been observed in reverse micelles (Figure 2A). However, the polydispersity remains rather large (Table 1). Thus, to reduce the polydispersity, the size-selected precipitation is used.

Size-Selected Precipitation (SSP). Size-selected precipitation is a well-known technique to separate mixtures of copolymers and homopolymers during the synthesis of sequenced copolymers.[22] It has been used[23,24] for extraction of nanosize nanocrystals elsewhere. This method is based on the mixture of two miscible solvents differing by their ability to dissolve the surfactant alkyl chains. The silver-coated particles are highly soluble in hexane and poorly in pyridine. Thus, a progressive addition of pyridine to hexane solution containing the

(22) In *Introduction àla Chimie Macromoléculaire*; Champetier, G., Monnerie, L., Eds.; Masson & Co,: Paris, 1969.
(23) Murray, C. B.; Noris, D. J.; Bawendi, M. G. *J .Am. Chem. Soc.* **1993**, *115*, 8706.
(24) Wilson, W. L.; Szajowski, P. F.; Brus, L. E. *Science* **1993**, *262*, 1242.

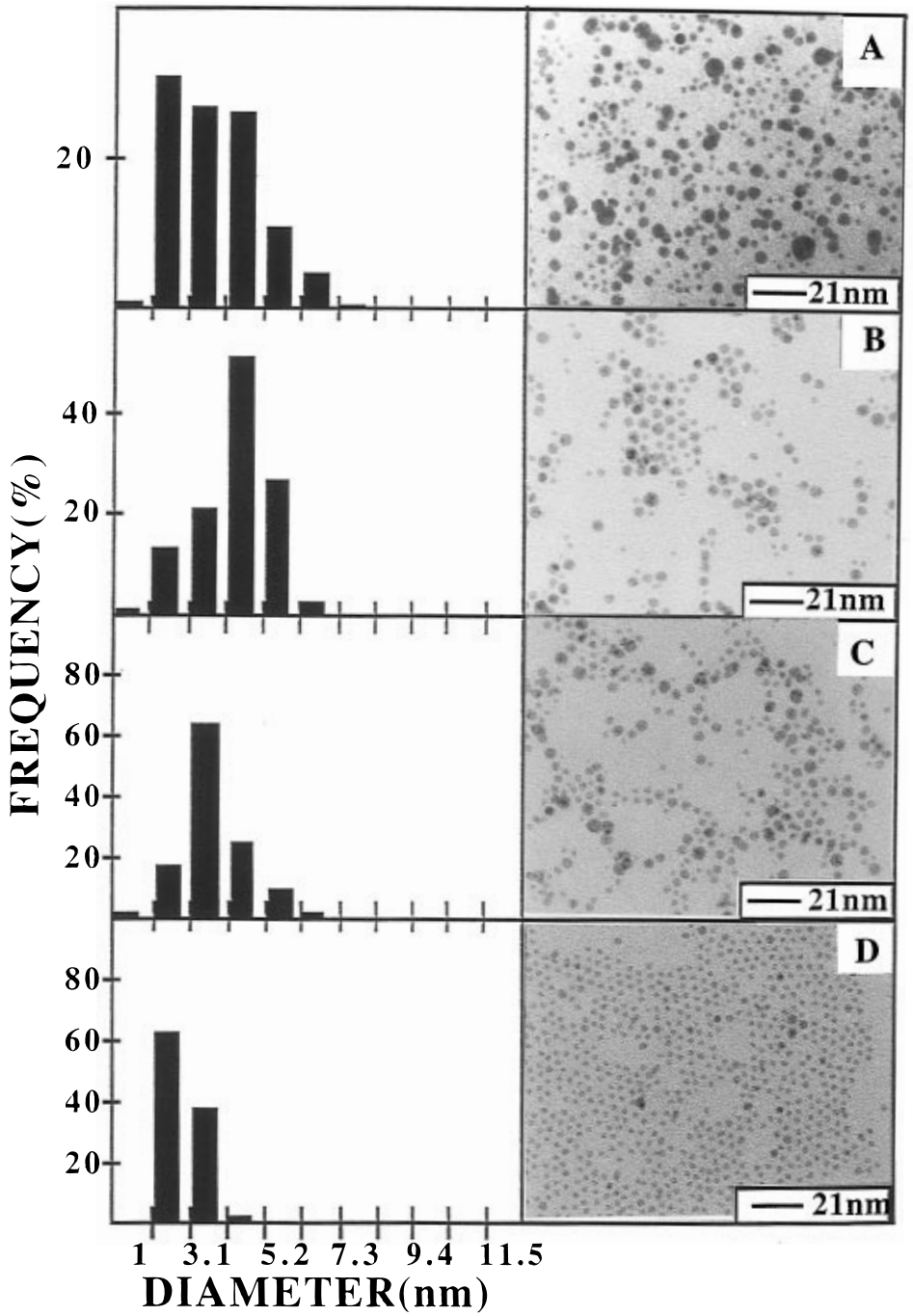

Figure 3. TEM micrograph and histograms of size of silver particles during the SSP process (number of fraction corresponds to the number of UV−Vis absorption spectra of Figure 4): (A) in reverse micelle; (B) fraction 1; (C) fraction 2; (D) fraction 3.

silver-coated particles is performed. At a given volume of added pyridine (which corresponds to roughly 50%), the solution becomes cloudy and a precipitate appears. This corresponds to agglomeration of the largest particles as a result of their greater van der Waals interactions.[7,11,24] The solution is centrifugated, and an agglomerated fraction rich in large particle is collected, leaving the smallest particles in the supernatant. The agglomeration of the largest particles is reversible and the precipitate, redispersed in hexane, forms a homogeneous clear solution. The TEM micrograph and histogram corresponding to the first precipitate are given on Figure 3B. They clearly show an increase in the average diameter and a decrease in the polydispersity (Table 2) compared to what has been observed before the size selection (Figure 3A). The same procedure as described above is performed with the supernatant, which contains the smallest particles. Pyridine is added to the supernatant until a precipitate is obtained. After centrifugation, the precipitate is dispersed in hexane. Figure 3C shows a decrease in the particles size and its distribution (Table 2). By repeat-

Table 2. Size Distribution of Silver Nanosized Particles at Different Steps of the Size-Selected Precipitation

sample	av diam (nm)	std dev (nm)	polydispersity (%)
initial after extraction	3.5	1.3	37
fraction 1	3.8	1	27
fraction 2	3	0.75	25
fraction 3	2.3	0.35	15

[a] The number of fraction refers to the absorption spectrum of Figure 4.

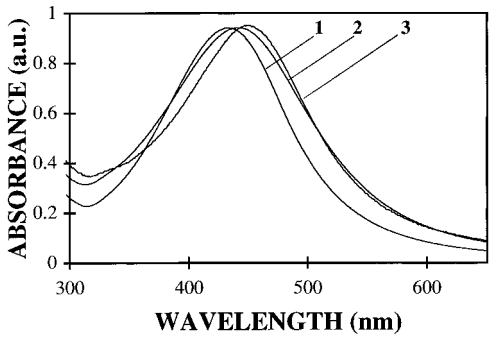

Figure 4. UV−visible absorption spectra of silver colloidal solution during the SSP process: Normalized spectra (at the maxima of the plasmon peak) showing the red-shift of the absorption fraction for each successive fraction (numbers refer to the order of fractionation).

ing the same procedure, very small particles are obtained (Figure 3D) with a very low polydispersity (15%). On the TEM micrograph (Figure 3D) a self-organization is observed. The silver nanosized particles form a hexagonal network with an average distance between particles equal to 2 nm.

The size selection can be followed by the absorption spectrum of silver particles dispersed in hexane. After each step, the absorption spectra of the precipitate redispersed in 1 cm^3 of hexane is recorded. Figure 4 shows the normalized UV−vis spectra corresponding to the various fractions during the process. A red-shift in the absorption spectrum with an increase of the number of fractions is observed. The particles dispersed in each of these solutions are observed by TEM. The particle size decreases as the number of fractions increases (Figure 3B−D). Hence, the red-shift of the plasmon band corresponds to a decrease in the average particle size (Table 2). This confirms the theoretical[19] and the experimental[12] investigations.

The sum of the absorption spectra of the various fractions is roughly the same as that observed before the SSP technique. This indicates that most of the material is recovered during the process.

Hence, by using the SSP technique, a strong decrease in the average diameter (from 3.5 to 2.3 nm) and a narrowing of the size distribution (from 37% to 15%) are observed. This decrease in the polydispersity favors spontaneous organization of nanosized silver particles. This can be attributed to an equilibrium between the van der Waals attractive forces and the repulsive hard-sphere interaction. Because these forces are isotropes, this equilibrium yields a compact organization in hexagonal bidimensional network. No 3D superlattice is observed. This is probably because the average diameter of silver particles is rather small (2.3 nm) and the van der Waals forces are not strong enough to induce the crystallization.

To get a 3D superlattice, a size-selected process is performed with coated particles obtained from the first SSP process (fraction 1) and dispersed in hexane (Figure 3B). Pyridine is added to the hexane solution until a precipitate appears. It is redispersed in hexane (in the SSP described above, this process is performed with the supernatant instead of the first precipitate redispersed in hexane). The size of the coated particles is then determined by SAXS experiments and is compared to that obtained by TEM.

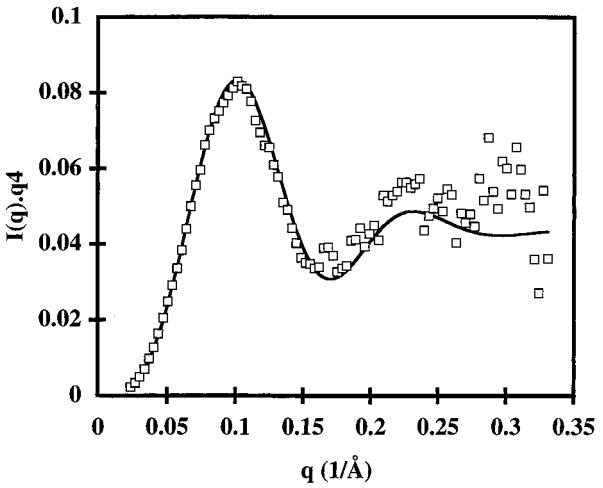

Figure 5. Small-angle X-ray scattering of the silver colloidal solution after complete treatment. Porods representation of the scattered intensity showing the pronounced oscillation characteristic of spherical and monodisperse particles. The solid line corresponds to the best fit obtained assuming spherical particles of silver with a Gaussian distribution of size.

Figure 5 shows the Porod representation of the scattered intensity obtained by SAXS on the solution containing the coated silver particles. The well-defined minimum and maximum confirm the very low polydispersity in size. Table 3 shows a similar average diameter deduced from Guinier and Porod plots. This confirms that the scatter is due to noninteracting spherical particles. The average diameter determined by SAXS is larger than that deduced from TEM experiments (see below). This is attributed to the scatter of the SH headgroup of the dodecanethiol used to coat the particles.

The TEM pattern and histogram (Figure 2C) show particles having an average diameter of the particles equal to 4.1 nm with a polydispersity equal to 12.5% (Table 1). In some part of the carbon grid, bidimensional self-organization takes place (Figure 7A). HR-TEM confirms the close-packing organization, and the high crystallinity of the silver particles (Figure 6). As expected, the particles are faceted. When the particles are closed packed, they are arranged in a hexagonal network (Figure 6). The average distance between two particles is equal to 2.1 ± 0.1 nm.

The length of the dodecanethiol tail, *l*, can be evaluated from the empirical equation given by[25]

$$l\,(\mathrm{nm}) = 0.25 + 0.127n$$

where *n* is the number of CH_2 groups ($n = 12$). The calculated value is found to be equal to 1.77 nm. The similarity between the interparticle distance (2.1 nm) and the length of the alkyl chain (1.77 nm) would imply a total interpenetration of the alkyl chains. This is impossible for steric considerations. However, the value of interparticle distance obtained in the present paper is similar to those obtained previously with silver sulfide[7] or gold[11] nanocrystals coated by dodecanethiol. These data can be explained in term of intercalation of individual chain or domains of chains in the zone where the chains are disordered. As a matter of fact, Badia

(25) Bain, C. D.; Evall, J.; Whitesides, G. M. *J. Am. Chem. Soc.* **1989**, *111*, 7155.

Table 3. Value of the Particles Diameter As Obtained by SAXS and TEM for Silver Particles after Complete Treatment (All Values in nm)

		SAXS adjustment		TEM	
Porod's diameter	Guinier diameter	diameter	polydispersity	diameter	polydispersity
5.2	5	4.8	15%	4.1	12.5%

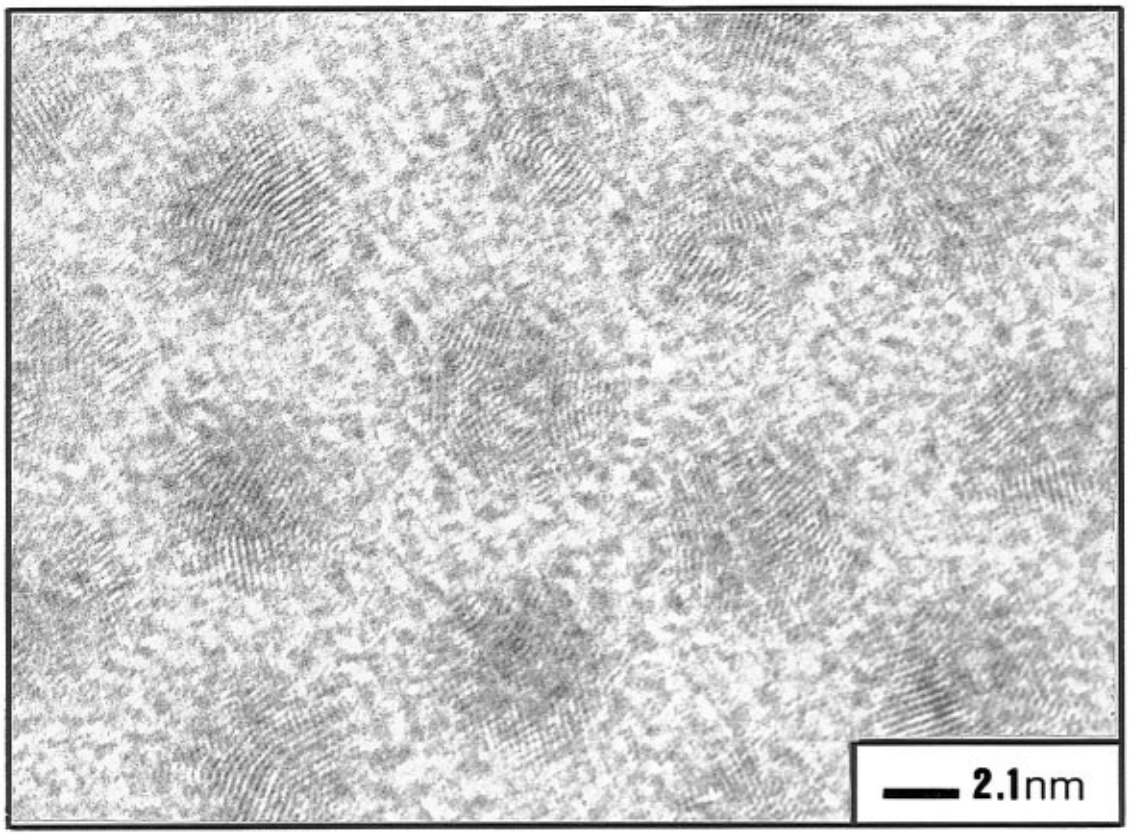

Figure 6. High-resolution TEM micrographs of silver particles after complete fractionation and deposition on a TEM grid.

et al.[26] demonstrated, by NMR, the coexistence of crystallized alkyl chain into an extended all-trans configuration and a smaller population of liquidlike conformationally disordered chains. Simultaneously, Luedtke et al.[27] show, by molecular dynamic simulations, the high order of surfactant groups used to coat the nanocrystal. The passivating dodecanethiol monolayer is "bundled" into groups of molecules with a preferential intermolecular orientation of the molecular backbones in each bundle. The bundles themselves are preferentially oriented regarding each other. Hence, from several facets of the single nanocrystals, the surfactant groups are bundled together into a single compact group. The similarity between the average interparticle distance and the length of the alkyl chain suggest that the close-packing alkyl chains into an all-trans conformation is achieved by intercalation or interpenetration of individual or domains of chains.

Three-Dimensional Self-Organization of Silver Nanosized Particles. To build a 3D self-organization, the above-described 4.1 nm diameter coated particles are dispersed in hexane. As described above, by leaving a drop of the solution on a TEM carbon grid, an imperfect organization (Figure 7A) is obtained. By leaving the carbon grid for 3 h in the solution, the TEM pattern is completely covered by a monolayer made of particles (Figure 7B). They are organized in a hexagonal close-packed network. In some region of the TEM pattern (Figure 7B), it can be observed a difference in the contrast. This can be attributed to a start of 3D self-organization. The increase of the immersion time until complete evaporation of the solvent yields to the formation of large aggregates. Figure 8A shows a rather high orientation of these aggregates around a large hole or ring. The average distance between the oriented aggregates varies from 20 to 60 nm. By varying the magnification of the aggregates (Figure 8B,C), it can be concluded that they are made of silver nanoparticles. The average size of these aggregates ranges from 0.03 to 0.55 μm^2. High magnification of one of these aggregates shows that the particles are arranged in two different symmetries. Figure 9 A shows the formation of a polycrystal. Magnification of Figure 9A (Figure 9B) shows either a hexagonal or a cubic arrangement of nanoparticles. The transition from one structure to another is abrupt, and there is a strong analogy with "atomic" polycrystals with a small grain called nanocrystals. Each domain or grain has a different orientation. This clearly shows that the stacking of nanoparticles is periodic and not random. The "pseudohexagonal" structure corresponds to the stacking of a {110} plane of the FCC structure (Figure 9C). On the same pattern it is observed (Figure 9B) a 4-fold symmetry which is

(26) Badia A.; Gao, W.; Singh, S.; Demers, L.; Cuccia, L.; Reven, L. *Langmuir* **1996**, *12*, 1262.
(27) Luedtke, W. D.; Landman, U. *J. Phys. Chem.* **1996**, *32*, 13324.

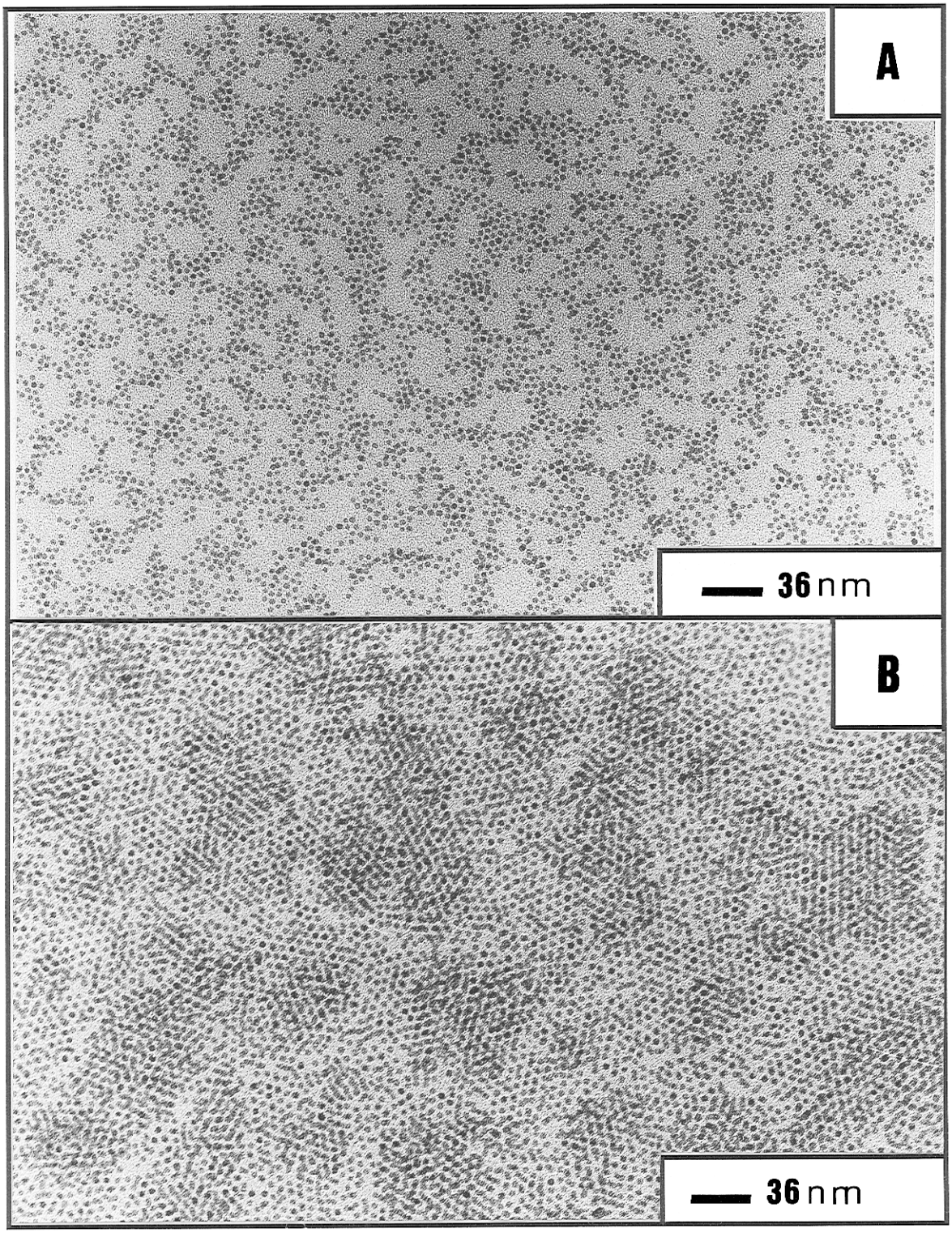

Figure 7. TEM micrographs of monolayers obtained by depositing a droplet of silver colloidal solution on a grid (A) or immerging for 3 h a TEM grid into the solution (B).

again characteristic of the stacking of {011} planes of the cubic structure and cannot be found in the hexagonal structure (Figure 9C). This is because there is no direction in a perfect hexagonal compact structure for which the projected positions of the particles could take this configuration. This is confirmed by TEM experiments performed at various tilt angles. By tilting the sample, it is always possible to find an orientation for which the stacking appears to be periodic. Hence by tilting a sample having a pseudo hexagonal structure, a 4-fold symmetry is obtained. From this information, it can be concluded that the large aggregates of silver particles are formed by stacking of monolayers in a face-centered cubic arrangement.

The cell parameter can be deduced from either the 4-fold symmetry or "hexagons". In the first case the cell parameter is found equal to 9 ± 1 nm. In a perfect crystal, the lattice of a hexagon corresponding to {1,1,0} plane is constant. On Figure 9B, the lattice varies and is found equal to $a = b = 9$ nm and $c = 6.6$ nm. This

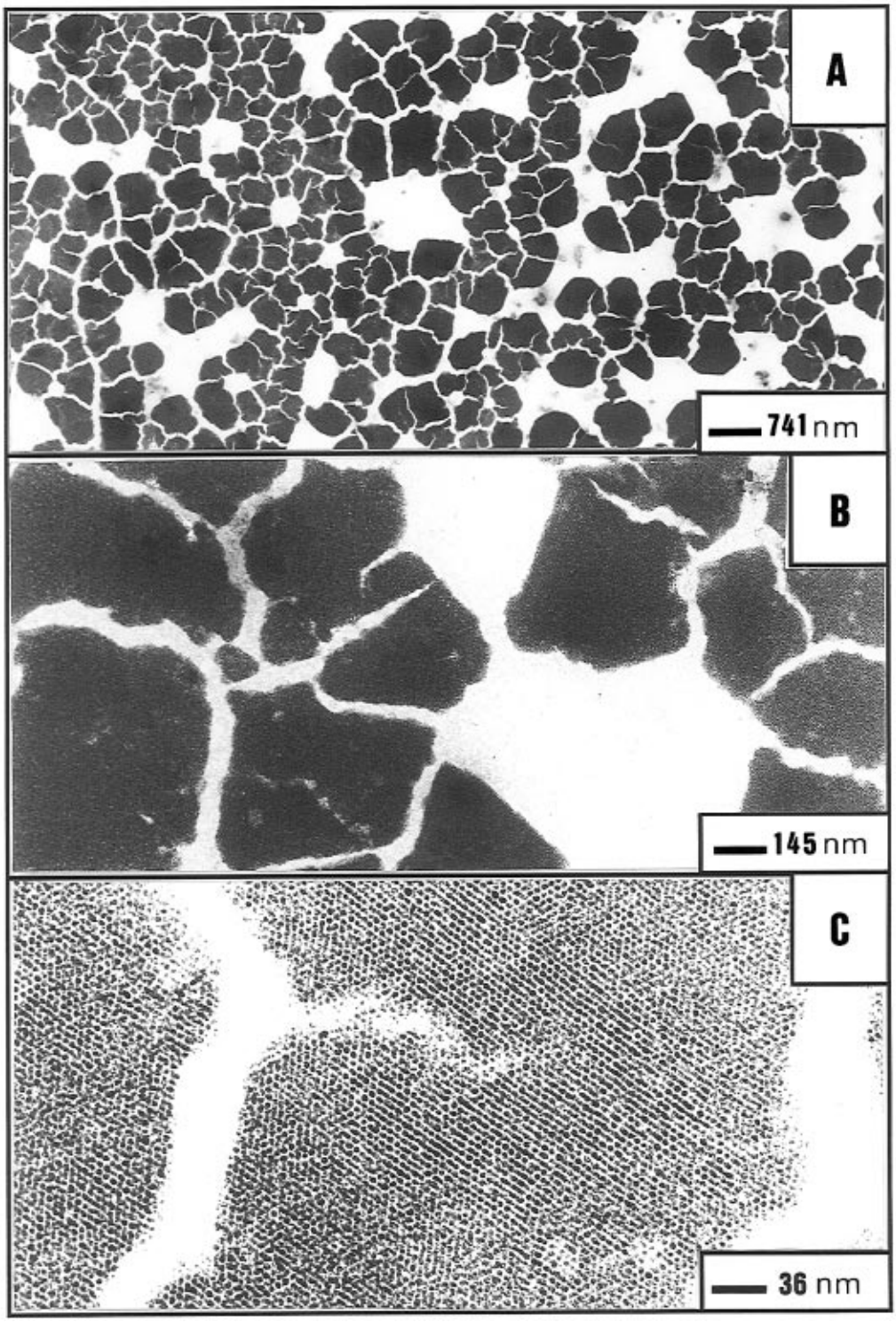

Figure 8. TEM micrographs obtained after immerging a TEM grid into the solution until complete evaporation of the solvent. A−C refer to different magnifications of the sample.

change on one of the lattices can be attributed to a distortion of the FCC structure. Very recently,[27] simulations of 3D superlattice made of gold particles coated with dodecanethiol reveal the formation of a tetragonally distorted FCC structure at room temperature. Hence, the appearance of a distorted structure can be observed and good agreement between the experimental data and the simulations is obtained.

The formation of a 3D lattice does not need any external forces. As mentioned before, it is due to van der Waals attraction forces and to repulsive hard-sphere interactions. These forces are isotropic, and the particle arrangement is achieved by increasing the density of the "pseudocrystal", which tends to have a close-packed structure. This imposes the arrangement in a hexagonal network of the monolayer. The growth in 3D could follow either a HC or FCC structure. The fact that a 4-fold structure is observed in Figure 9B excludes the possibility of having a HC structure, and it can be concluded that the 3D supperlattice has a FCC structure (Figure 9C). It is important to note than these crystals are obtained spontaneously only by decreasing the polydispersity of silver particles synthesized in situ in AOT reverse micelles.

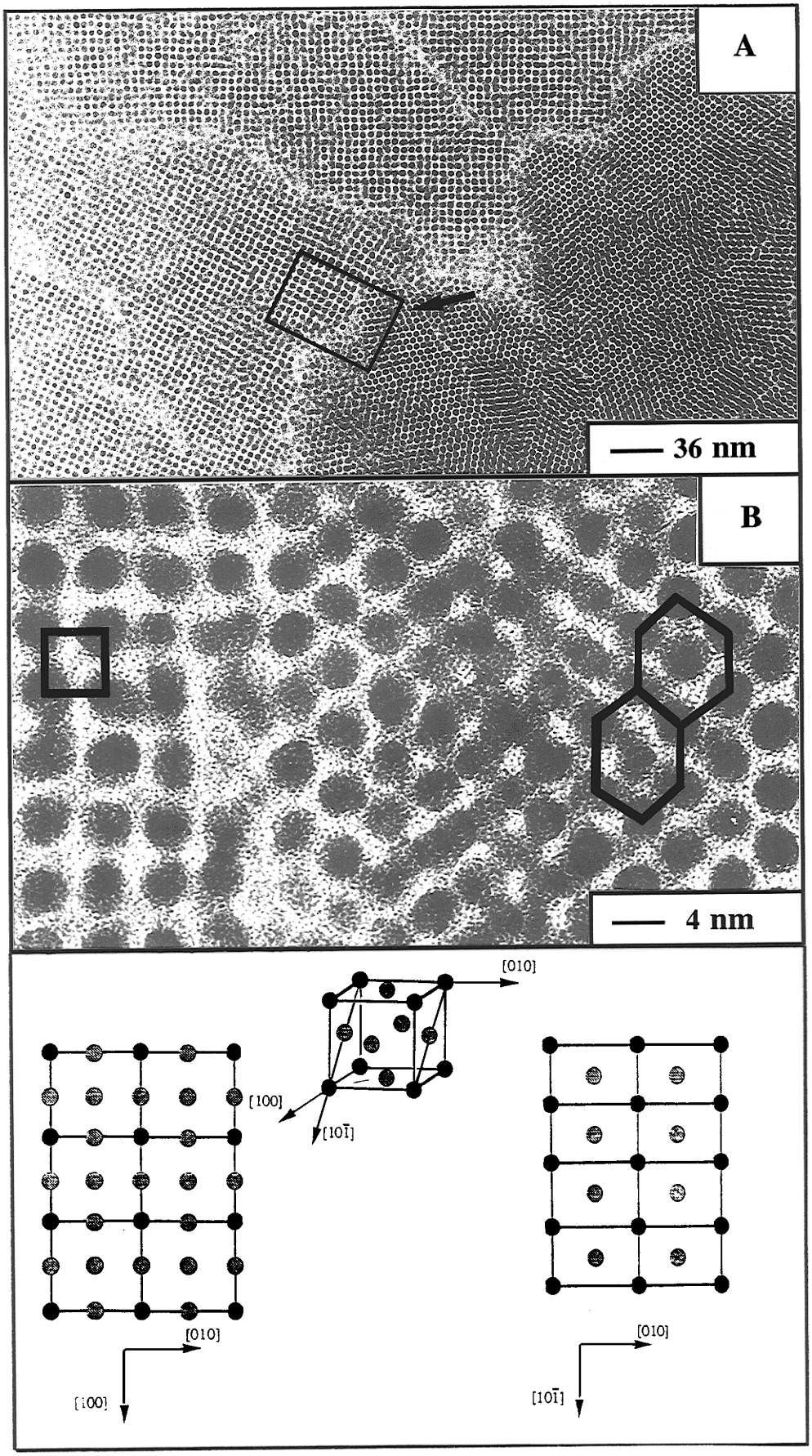

Figure 9. TEM micrograph of the grid at high magnification showing the different orientation of the silver particle: (A) general view, (B) magnification of the indicated region; (C) schematic representation of the different orientation observed assuming a fcc structure of the nanocrystal.

Conclusion

Functionalized AOT reverse micelles allows us to obtain easily, by simple mixing, calibrated nanosized silver particles in solution. However, the polydispersity is high, similar to that of AOT reverse micelles. To decrease this polydispersity, extraction and fractionation of the silver particles were undertaken. This allows us to narrow the size distribution from 43% to 12.5%. Immersing a support in a solution of silver particles yields, simply by changing the immersion time, the formation of a 2D hexagonal network of silver particles or a large microcrystal of silver particles with a FCC arrangement. Thus, it is now possible to determine the dependence of the electrical, optical, and electrooptical properties of this crystal of nanosized particles with the interparticles distances.

Acknowledgment. The authors thank Dr. J. Douin for the TEM Tilts experiments and for fruitful discussion, M. Lavergne for all the TEM experiment, and Dr. M. Olvera de la Cruz for critical reading of the manuscript.

CM960513Y